IEEE Photonics Journal
An IEEE Photonics Society Publication

Open Access

# Toward Self-Similar Propagation of Optical Pulses in a Dispersion Tailored, Nonlinear, and Segmented Bragg-Fiber at 2.8 $\mu$m

Volume 9, Number 4, August 2017

**Piyali Biswas**
**Bishnu Pada Pal**, ***Senior Member, IEEE***
**Abhijit Biswas**, ***Member, IEEE***
**Somnath Ghosh**

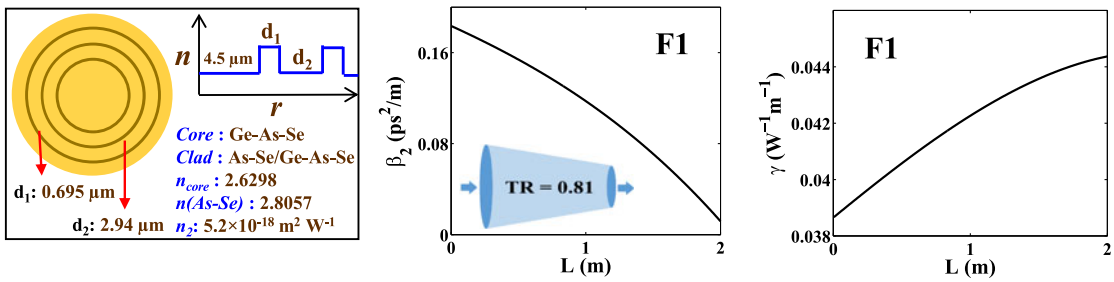


(a) (b) (c)

DOI: 10.1109/JPHOT.2017.2731870
1943-0655 © 2017 IEEE

# Toward Self-Similar Propagation of Optical Pulses in a Dispersion Tailored, Nonlinear, and Segmented Bragg-Fiber at 2.8 $\mu$m

**Piyali Biswas,[1] Bishnu Pada Pal,[2] *Senior Member, IEEE*, Abhijit Biswas,[1] *Member, IEEE*, and Somnath Ghosh[3]**

[1]Institute of Radio Physics and Electronics, University of Calcutta, Kolkata 700009, India
[2]Department of Physics, Bennett University, Greater Noida 201310, India
[3]Department of Physics, Indian Institute of Technology, Jodhpur 342011, India

*DOI:10.1109/JPHOT.2017.2731870*


Manuscript received May 9, 2017; revised July 20, 2017; accepted July 21, 2017. Date of publication July 23, 2017; date of current version August 22, 2017. This work was supported by the Department of Science and Technology India under INSPIRE Faculty Fellow scheme (IFA-12; PH-23) and in part by the Department of Navy (USA) Grant issued by ONRG (N62909-10-1-7141). Corresponding author: Somnath Ghosh (e-mail: somiit@rediffmail.com).

**Abstract:** We demonstrate self-similar stable propagation of parabolic optical pulses through a highly nonlinear specialty Bragg fiber at 2.8 $\mu$m by a numerical approach. To obtain such propagation characteristics over a longer length of a Bragg fiber, we propose and verify a fiber design scheme that underpins passive introduction of a rapidly varying group-velocity dispersion around its zero dispersion wavelength and modulated nonlinear profile through suitable variation in its diameter. To implement the proposed scheme, we design a segmented and tapered chalcogenide Bragg fiber in which a Gaussian pulse is fed. Transformation of such a launched pulse to a self-similar parabolic pulse with full-width-at-half-maxima of 4.12 ps and energy of $\sim$39 pJ is obtained at the output. Furthermore, a linear chirp spanning across the entire pulse duration and 3 dB spectral broadening of about 38 nm at the output are reported. In principle, the proposed scheme could be implemented in any chosen set of materials.

**Index Terms:** Fiber nonlinear optics, pulse shaping.

## 1. Introduction

Nonlinear propagation of high power optical pulses at the mid-infrared (mid-IR) ranging from 2 to 25 $\mu$m has become an exciting area of research in science and technology due to its potential applications particularly in defence, biomedical surgery, supercontinuum (SC) generation, micro-machining, spectroscopic molecular finger printing, chemical/bio-molecular sensing, weather forecasting and so on [1]–[4]. Such applications require efficient mid-IR pulsed laser sources and suitable light-guiding structures. Silica made fibers are not useful in mid-IR wavelength range due to their high absorption loss. Hence, the urgent need of suitable mid-IR optical fibers has propelled the development of most potential candidate in this regime namely chalcogenide glass materials (i.e., glasses containing cations of S, Se, Te) which exhibit excellent linear and nonlinear properties. Moreover, post-processed less toxic nature of such glasses makes them useful for biomedical diagnosis. However, presence of high Kerr nonlinearity in such glasses (value of $n_2$ 1000 times

larger than that of silica) makes the optical fibers compulsorily highly nonlinear [5] which in turn deviates the dynamics of optical pulse propagation through them from the standard one. Recent developments on mid-IR lasers and availability of fabrication-compatible low-loss nonlinear infrared (IR) glasses have been driving further studies on nonlinear pulse propagation in the IR wavelength range [6]–[8]. Usually, dynamics of any nonlinear systems in physics require solving a set of similar kind of certain complex partial differential equations. For a simplified approach to study nonlinear pulse propagation, one often exploits symmetry techniques to obtain a self-similar kind of solutions to these equations [9]. Nonlinear Schrödinger equation (NLSE) governs nonlinear electromagnetic wave propagation in fiber optics, solution of which in the normal group velocity dispersion (GVD) regime is asymptotically self-similar, whose temporal power profile is parabolic in shape [10], [11]. Such self-similar parabolic solutions of NLSE have tremendous capability of tolerating large nonlinearity without suffering wave breaking [12]. Furthermore, increasing demand of ultra-short, high power pulse propagation in various applications have attracted considerable attention to researchers toward self-similar propagation. Ultra-short high power pulses propagating through a nonlinear medium often suffer from the deleterious effect of optical wave breaking (OWB) due to accumulation of large nonlinear phase shift and interference effect during pulse propagation [13]. Also, investigations have revealed that OWB can be promisingly avoided by formation of self-similar parabolic pulses (PP) with linear chirp across its width. To date, several studies have been reported in the literature on the formation of PPs, in both active and passive fibers [14]–[21]. However, recent investigations have revealed that PPs that are formed in highly nonlinear and passive fibers (mainly chalcogenide fibers), are unable to reach steady state condition of propagation after formation due to excessive nonlinearity that overshadows the dispersion. As a result, the parabolic temporal pulse profile gradually reshapes itself into a nearly rectangular profile and eventually leading to OWB. Hence, the so formed PPs are *merely intermediate transient state* of propagation and eventually fail to retain its *acquired self-similarity* over longer propagation length [18], [22]. Very recently, in this direction some studies have been reported on pulse propagation in highly nonlinear and dispersion decreasing microstructured optical fibers (MOF) where the self-similar propagation of PPs is limited to a few centimeters. It was also established that pulse propagation in this regime is independent of the choice of fiber's dispersion profile and prone to instabilities [23]. In order to address the challenge in realizing high power parabolic pulses through highly nonlinear fibers, it is worthwhile to quantify the *soliton order N* that inherently include the peak power of the input pulse. On the basis of few reports in [24], [25], self-similar PPs are realizable in passive fibers with $N \leq 10$ over longer distances whereas the same is difficult in fibers with $N \gg 10$ as in the cases of chalcogenide glass made fibers. Thus for our targeted applications in the mid-IR wavelength range such as high power delivery [2], [3], [26], and SC-generation at mid-IR [1] necessitate novel schemes for designing specialty fibers to address the specific difficulty of high power PP propagation over longer distances through nonlinear media [27]. To address this state-of-the-art challenge, we propose a new scheme. The motivation of our proposed fiber scheme and the design based on it is to achieve self-consistent parabolic pulses evolved from some initial pulse with higher intensity and much shorter/ultrashort pulse duration over much longer distances at mid-IR.

In this work, we propose a specialty Bragg fiber design eventually independent of choice of fiber materials available at mid-IR, whose dispersion profile has been unconventionally tailored for attainment of self-similarity with propagation in a highly nonlinear medium, and numerically demonstrate the propagation of self-similar parabolic pulses through such a highly nonlinear and passive Bragg fiber at the mid-IR wavelength of 2.8 $\mu$m. For this purpose, we choose suitable chalcogenide glasses for designing the Bragg fiber: *GeAsSe* as the low index core material and combination of *AsSe/GeAsSe* as the cladding material. In order to obtain self-similar propagation for the formed PPs, we employ a rapidly varying GVD profile with a mean value close to zero so that the effect of dispersion induced phase shift on pulse in such a segmented highly nonlinear Bragg fiber (HNBF) can be reduced significantly. Formation of high power PPs through self-similar propagation over long lengths of the designed HNBF is reported. Characteristic temporal and spectral broadening of PPs are also shown with proper linear chirp across the pulse width.

## 2. Numerical Model

Parabolic pulses with linear chirp across its width are formed through interplay between nonlinear phenomenon of self phase modulation (SPM) and positive GVD. In highly nonlinear passive fibers, primarily nonlinearity drives the dynamics of such PPs overshadowing dispersion and hence fails to attain self-similarity. In order to study the dynamics of ultra-short pulse propagation through a dispersion and nonlinearity tailored HNBF, we need to solve the nonlinear Schrödinger equation (NLSE) numerically for a slowly varying picosecond (ps) pulse envelope $A(z, t)$ [28].

In an ideal loss-less optical fiber in the normal GVD regime i.e., where value of GVD parameter $\beta_2$ is positive for a hyperbolic dispersion decreasing profile along length of the fiber, the asymptotic solution of NLSE yields a parabolic intensity profile. Under this condition, the propagation of optical pulses is governed by the NLSE of the form

$$i\frac{\partial A}{\partial z} - \frac{\beta_2}{2}D(z)\frac{\partial^2 A}{\partial T^2} + \gamma(z)|A|^2 A = 0, \tag{1}$$

where $\beta_2$ (GVD parameter) $> 0$ at $z = 0$, $D(z)$ is length dependent dispersion profile due to tapering with $D(0) = 1$ and customized according to our proposed scheme, and $\gamma(z)$ is longitudinally varying nonlinear (NL) coefficient. Initially, we have neglected the third order dispersion (TOD) effect during pulse propagation, and thus have excluded the term relating TOD from (1). The dispersion and nonlinear parameters i.e., $\beta_2$ and $\gamma$ are calculated along the propagation length of the segmented HNBF at the central wavelength of 2.8 $\mu$m. With the use of coordinate transformation $\xi = \int_0^z D(z')dz'$ and defining a new amplitude $U(\xi, T) = \frac{A(\xi,T)}{\sqrt{D(\xi)}}$, (1) transforms to

$$i\frac{\partial U}{\partial \xi} - \frac{\beta_2}{2}\frac{\partial^2 U}{\partial T^2} + \gamma(z)|U|^2 U = i\frac{\Gamma(\xi)}{2}U, \tag{2}$$

where,

$$\Gamma(\xi) = -\frac{1}{D}\frac{dD}{d\xi} = -\frac{1}{D^2}\frac{dD}{dz}. \tag{3}$$

Equation (3) clearly indicates that $D(z)$ is a decreasing function of $z$. Hence decreasing dispersion acts exactly as $z$-dependent gain term in (2) mimicing a length dependent fiber amplifier with normal GVD. For specificity, if we choose $D(z) = \frac{1}{1+\Gamma_0 z}$, the gain coefficient becomes constant, i.e., $\Gamma = \Gamma_0$. Here, in the normal GVD regime, for the chosen dispersion profile, and for a constant gain coefficient, the NLSE yields an asymptotic self-similar parabolic solution with a linear-chirp across its width. The chirp developed is the time dependence of the instantaneous frequency $\omega$ and is computed using the relation,

$$\delta\omega(T) = -\frac{\partial\phi}{\partial T}, \tag{4}$$

where $\phi$ is the accumulated phase shift for both dispersion and nonlinearity simultaneously. For subsequent discussion in this paper, it is convenient to use representative notations $L_D$ as the dispersion length, $L_{NL}$ the nonlinear length and $N$ as representing soliton number:

$$L_D = \frac{T_0^2}{|\beta_2|}, \qquad L_{NL} = \frac{1}{\gamma P_0}, \qquad and \qquad N = \sqrt{\frac{L_D}{L_{NL}}}. \tag{5}$$

where $P_0$ is the peak power of the initial pulse, $T_0$ is the initial pulse duration (half-width at $1/e$ intensity point). Equation (2) has been solved by Split-Step Fourier Method (SSFM) which is possibly the easiest and fastest way to solve the NLSE numerically [28].

In order to check the quality of the evolved parabolic pulse, we compute the evolution of the misfit parameter ($M$) between the pulse temporal intensity profile $|U|^2$ and the parabolic fit $|p|^2$ of the

same energy defined as [21]

$$M^2 = \frac{\int [|U|^2 - |p|^2]^2 dT}{\int |U|^4 dT}, \tag{6}$$

where the expression for the parabolic fit with peak power $P_p$ and pulse duration $T_p$ is given by:

$$p(T) = \begin{cases} P_p(1 - \frac{T^2}{T_p^2}) \text{ for } |T| \leq |T_p| \\ 0 \text{ for } |T| > |T_p| \end{cases} \tag{7}$$

The smaller value of $M$ indicates the better fit to the targeted parabolic waveform. We have considered $M$ <0.04 which is sufficient for a pulse to be parabolic.

Moreover, we have chosen picosecond pulses for the study of pulse propagation, which are said to be free from higher order nonlinear effects such as SRS, TPA, etc. [29]. Thus, initially we have not incorporated the term relating such higher order nonlinearities into our computation. Later, we have considered such higher order nonlinear terms (e.g., SRS and TPA coefficients) along with the term relating TOD into the computation for better accuracy of the results and NLSE takes the form,

$$\frac{\partial U}{\partial z} = -\frac{\alpha}{2}U - i\frac{\beta_2}{2}\frac{\partial^2 U}{\partial T^2} - \frac{\beta_3}{6}\frac{\partial^3 U}{\partial T^3} + i\left(\gamma(z) + i\frac{\alpha_2}{2A_{eff}}\right)\left(1 + \frac{i}{\omega_0}\frac{\partial}{\partial T}\right)U\int_{-\infty}^{\infty} R(T)U dT, \tag{8}$$

where, $\beta_3$ is the third order coefficient and $R(T) = (1 - f_R)\delta T + f_R h_R(T)$ is the response function including the Raman response function

$$h_R(T) = \frac{\tau_1^2 + \tau_2^2}{\tau_1 \tau_2^2}\exp(-T/\tau_2)\sin(T/\tau_1). \tag{9}$$

Here, $f_R$ is the Raman response, $\tau_1$ and $\tau_2$ have their usual meanings. The term $\gamma(z) + i\frac{\alpha_2}{2A_{eff}}$ accounts for the nonlinear loss due to TPA where $\alpha_2$ is the TPA coefficient.

## 3. Fiber Design Scheme

In order to achieve self-similar propagation, we propose a new method based on a suitable dispersion and nonlinearity tailoring in highly nonlinear media along the propagation length. The scheme is endowed with a rapid variation of dispersion and nonlinearity over the propagation length. Specifically, the dispersion varies rapidly along the fiber length around a positive mean value, while the fiber nonlinearity correspondingly gets simultaneously modulated (due to its $z$-dependence) around a high value of $\gamma$. Recently, some works have been reported where specific fiber designs are adopted in order to achieve self-similar PPs [30], [31]. To implement the proposed scheme, we target to design a specialty optical fiber to support self-similar parabolic pulse at 2.8 $\mu$m in the mid-IR wavelength range. The availability of laser source at 2.8 $\mu$m has driven us to design a parabolic pulse source at this mid-IR wavelength. Furthermore, fabrication-compatible chalcogenide glasses at mid-IR are highly nonlinear in nature. To meet the challenges to form self-similar pulses in such fibers, we design two HNBFs with customized dispersion and nonlinear profiles.

Initially, we have designed a dispersion decreasing Bragg fiber (DDBF) for PP formation, where light is guided by the designed PBG around the chosen wavelength. To achieve this, we have considered two chalcogenide glass materials namely, (a) *GeAsSe* having a refractive index of 2.6298, and (b) *AsSe* with a higher refractive index of 2.8057, both at 2.8 $\mu$m. The thermal conductivity of *GeAsSe* core is 0.18 W/m.K which is lower than that of the cladding material *AsSe* (0.24 W/m.K) exhibitting a good thermal compatibility of the two, as generated heat would easily be dissipated through the cladding structure. Moreover, other physical parameters of the two materials are in good agreement to have better thermo-mechanical compatibility [32]–[34]. The designed HNBF consists of *GeAsSe* core of radius 4.5 $\mu$m surrounded by three successive bi-layers of cladding thereby forming the desired PBG. Here, a cladding bi-layer consists of a high-index *AsSe* layer of width $d_1$

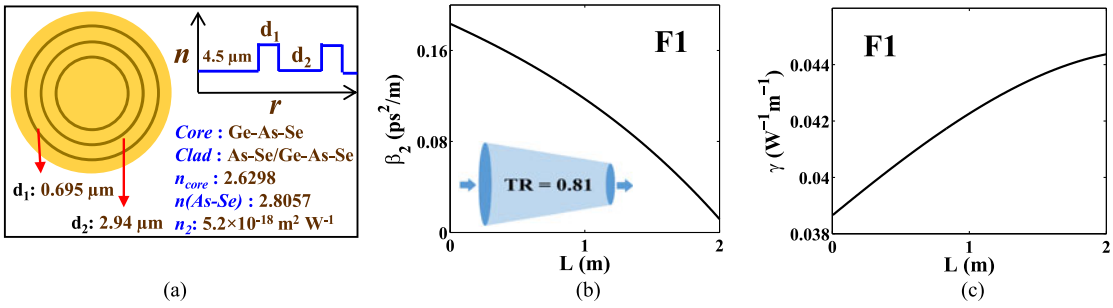


Fig. 1. (a) Input cross-section with refractive index profile of the designed photonic Bragg fiber F1; variation of (b) GVD parameter ($\beta_2$) and (c) nonlinear parameter ($\gamma$) along the length of F1.

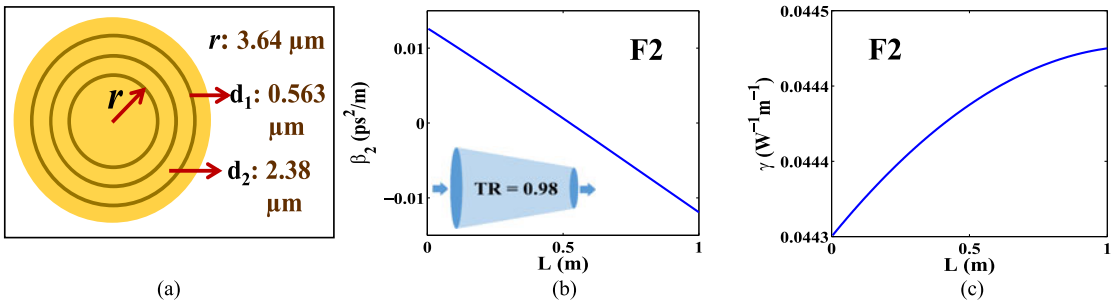


Fig. 2. (a) Input cross-section of the 1 m long designed HNBF F2 with its dimensions; longitudinal variations of (b) GVD parameter ($\beta_2$), and (c) nonlinear parameter ($\gamma$) for F2.

along with a low-index *GeAsSe* layer of width $d_2$. The nonlinear refractive index $n_2$ of the core material is very high, $\sim 5.2 \times 10^{-18} \text{m}^{-2}/\text{W}$ at 2.8 $\mu$m. We refer to this designed HNBF as F1 as shown in Fig. 1(a). For F1, the value of GVD parameter $\beta_2$ is $1.8 \times 10^{-1}\ p\text{s}^2\text{m}^{-1}$ and nonlinear parameter $\gamma$ is $3.8 \times 10^{-2}\ \text{W}^{-1}\text{m}^{-1}$, both at 2.8 $\mu$m. Further, starting with these parameter values, F1 is assumed (in our design) to be down-tapered with a taper-ratio 0.81 over a length of 2 m. The output end cross-sectional parameters of F1 are (i.e., at 2 m): core-radius $r = 3.64\ \mu$m, $d_1 = 0.56\ \mu$m, $d_2 = 2.38\ \mu$m, $\beta_2 = 1.26 \times 10^{-2}\ p\text{s}^2\text{m}^{-1}$, and $\gamma = 4.43 \times 10^{-2}\ \text{W}^{-1}\text{m}^{-1}$. The longitudinal dependences of $\beta_2$ and $\gamma$ for F1 are shown in Fig. 1(b) and (c), respectively.The other HNBF, denoted as F2, is 1 m long with the same material as mentioned above keeping the input-end cross-section identical to the output-end cross-section of F1 in order to avoid any discontinuity in parameter values. F2 is down tapered with a taper-ratio of 0.98, so that the value of $\beta_2$ starts from positive, crosses zero value and reaches negative dispersion regime. Previously, existence of of PPs in negative dispersion regime has already been reported [35]. Now this specific dispersion profile of F2 is repeated in such a way over the next few meters in order to realize a rapidly varying periodic dispersion profile with a nearly mean-zero $\beta_2$ value. Such a dispersion tailoring in F2 is deliberately exploited in order to customize the dispersive effect of fiber on pulse propagation (along with associated modulation in $\gamma$) so as to achieve self-similarity of the formed PP. The cross-section of F2 is shown in Fig 2(a). Moreover, the longitudinal variations of $\beta_2$ and $\gamma$ are depicted in Fig. 2(b) and (c), respectively. The entire dispersion profile of the proposed segmented fiber with both F1 and F2 connected together following the proposed scheme are illustrated in Fig. 3(a). Corresponding variation of $\gamma$ is shown in Fig. 3(b) for the segmented HNBF over an arbitrarily chosen length of 8 m. In this context, the down taper-ratios assumed in our designed fiber were 0.81 and 0.98, which have been reported by other researchers [36], [37]. An experimental evidence of the down-tapering of an *AsSe* was reported in [38], [39] though not for *GeAsSe*. Since both these are thermally compatible chalcogenide glasses for stack and draw, we are optimistic that such taper ratios should be achievable in our designed fibers, if and when gets fabricated. In the proposed fiber design, the dispersion curve has crossed the zero dispersion value several times and hence the impact of third order dispersion (TOD) may have a

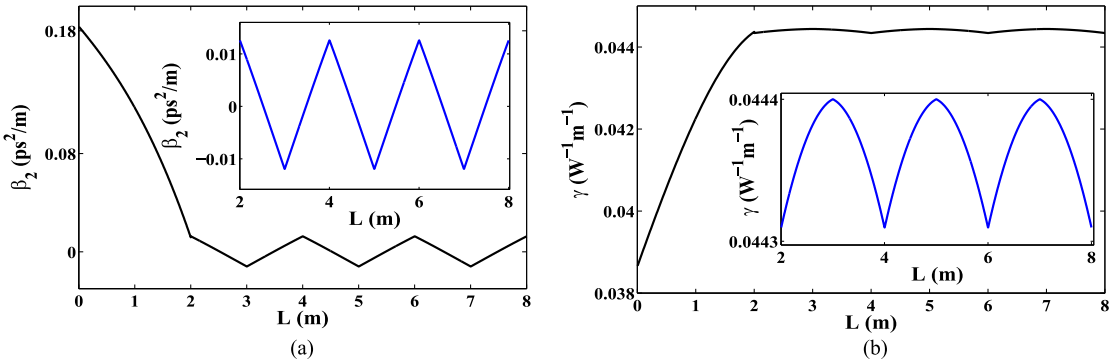


Fig. 3. (a) Variation in $\beta_2$ along the proposed segmented fiber over a length of 8 m. The initial 2 m length of F1 is combined with next six alternatively up-down segmented F2. Inset shows the variation in $\beta_2$ of alternating F2 over length; (b) variation in $\gamma$ along the total length of the proposed HNBF. Zoomed view of the $\gamma$ profile over alternating F2 only is shown as inset.

strong effect on pulse propagation, as previously it has been shown that in a dispersion decreasing fiber (DDF), when the ratio of TOD length $L_D^{'}$ to $L_D$ (i.e., $L_D^{'}/L_D$) is much greater than unity, it limits the stable propagation length of the pulse leading to asymmetric broadening and oscillations in both temporal and spectral domains [25], [40]. In the present work, for simplicity we have neglected the value of TOD and its impact on pulse propagation which will not be negligible in practice and later discussed separately in the next section. Further, the impact of TOD can be minimized by a suitable fiber design scheme. The proposed rapid dispersion variation along with nonlinearity modulation over length could be otherwise achieved by a single fiber with simultaneous up-and-down tapering. However, fabrication of such structures using chalcogenide glasses via state-of-the-art fabrication processes may be somewhat challenging [41]. Hence from the view-point of easier fabrication, we have designed the segmented fiber consisting of a 1 m long HNBF with zero-crossing longitudinal dispersion profile that can be spliced with another identical fiber tapered reversely and the process could be continued over longer distances with some compromise in loss penalty. In this context, a Bragg fiber is essentially a 1D equivalent of microstructured optical fibers/PCFs. Since splicing, tapering and jointing of microstructured fibers are no longer an insurmountable technical issue [42] and as the Bragg fiber cross-section has a simple core-clad structure, so we believe that there will be no major technical issues in successful splicing of such fibers with standard state-of-the-art equipment as and when such fibers of our design would be experimentally realized.

## 4. Results and Discussions

In our study, we considered an un-chirped Gaussian shaped initial pulse centered at the wavelength of 2.8 $\mu$m, from a mode-locked $Er^{3+}$-doped ZBLAN fiber laser as the optical source [43]. We have considered the peak power of the initial pulse to be 150 W and full-width-at-half-maximum (FWHM) to be 2.0 $p$s. The initial pulse with energy 0.3 nJ (as calculated) was assumed to be injected at the input end of the segmented HNBF and propagated down the entire fiber length of 8 m. In this context, all computations regarding the fiber design and pulse propagation were carried out for the only supported fundamental mode.

To understand the pulse dynamics, we analyze the results obtained both qualitatively as well as quantitatively. The overall pulse evolution is depicted in Fig. 4(a). Our findings reveal that after propagating only 1.5 m from the input end of the HNBF, Gaussian pulse starts evolving toward parabolic intensity profile in the time domain. Misfit parameter ($M$) computation for pulse evolution dictates that at 1.55 m from the input end of the HNBF, PP has been evolved with the minimum value of $M = 0.0179$. The misfit parameter $M$ evolution over length is shown as inset of Fig. 4(a). Explicit numerical study of the propagation dynamics reveals that once PP is formed in the HNBF, it maintains its shape over rest part of the length of the designed segmented HNBF. At the output end

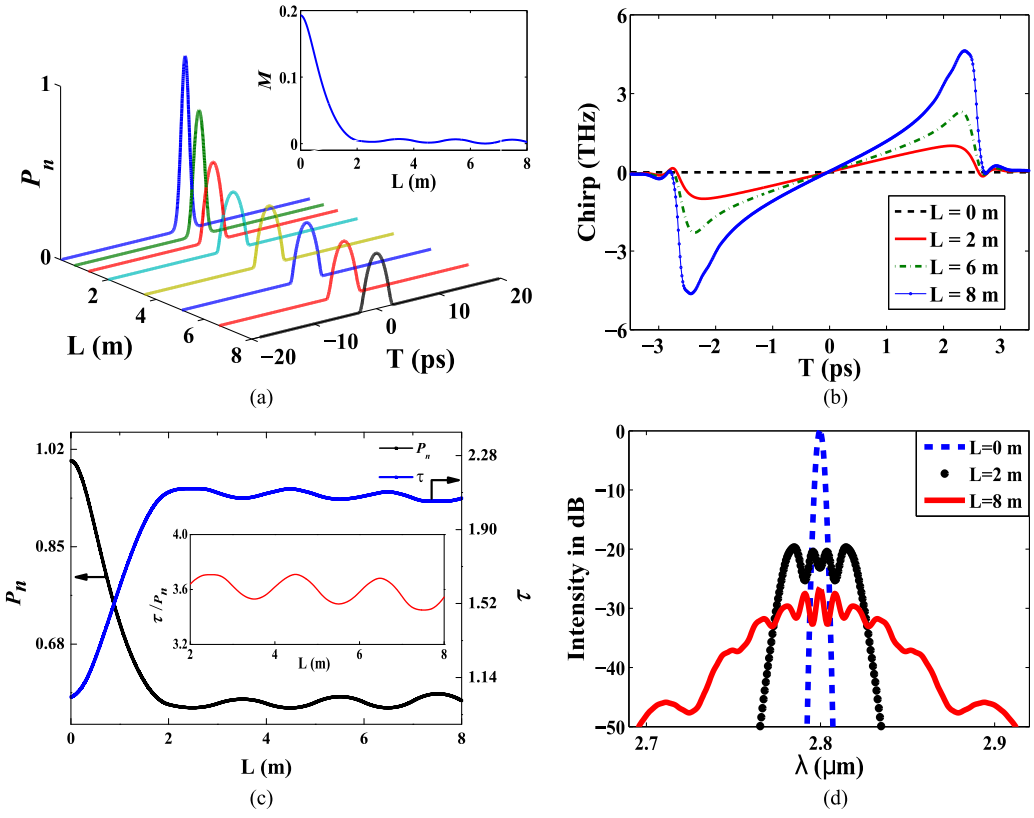


Fig. 4. (a) Evolution of self-similar pulses through the entire length of the segmented HNBF. Evolution of $M$ over length in the inset; (b) variation of chirp developed at different HNBF lengths; (c) variation in normalized pulse power ($P_n$) and normalized FWHM ($\tau$) against fiber length; also variation of the ratio $\tau/P_n$ with fiber length in the inset; and (d) variation of spectral intensity with wavelength for different fiber lengths.

of the fiber, a smooth self-similar PP with FWHM 4.12 $p$s and energy ~39 $p$J has been observed with a linear chirp across its width. In this context, mid-IR laser sources delivering femtosecond pulses with energy in the order of nano-Joules [27], mid-IR supercontinuum sources spanning over wide ranges of wavelength with much higher peak power [44]–[46], etc. have already been reported in literature. As our fiber design is new, it can be further optimized in order to obtain much higher power and shorter pulse widths competing efficiently with the existing mid-IR sources. Corresponding variation in chirp for different propagation lengths is shown in Fig. 4(b). It is evident that starting from an un-chirped condition, the chirp developed at 2 m of HNBF length from the input end has a perfect linear nature without oscillations across the entire width of the pulse. With further propagation, the linearity of the chirp is restricted to the center portion of the entire pulse duration with a sharp change at the edges. It can be explained as an effect of increasing accumulation of nonlinear phase-shifts due to steeper leading and trailing edges, though ringing/pulse oscillations have not appeared yet. Moreover, outside the pulse duration chirp computation has been possible due to the presence of very small but non-zero values of the pulse, since in practice no pulse drastically drops to zero at its edges but gradually acquires the zero. We have also computed the variation in pulse width $\tau$ (normalized) and normalized power $P_n$ with HNBF length along with their ratio $\tau/P_n$.

In Fig. 4(c), we have shown the simultaneous variation of normalized pulse power ($P_n$) and normalized FWHM ($\tau$) along the entire fiber length which clearly exhibit their complementary nature. To confirm the self-similar behavior of PP, we have shown the variation of $\tau/P_n$ over 6 m of HNBF length in the inset of Fig. 4(c). Our computed results show that the variation in $\tau/P_n$ has an average

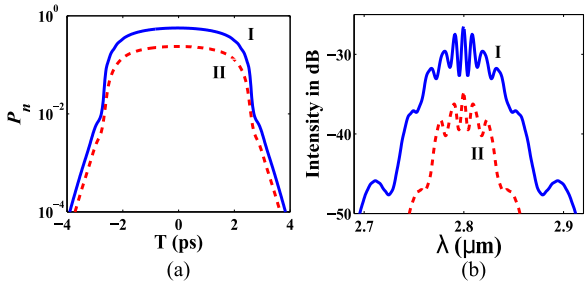


Fig. 5. (a) Temporal intensity profile (in logarithmic scale) of the output pulse and (b) spectral profile of the output pulse with (I) confinement loss only (blue solid curve) and (II) confinement, material and splice loss (red dashed curve).

of 3.595 with a standard deviation (SD) as low as 2.28%, which effectively implies a nearly constant variation over the chosen fiber length thereby establishing the self-similar nature of the evolved pulse. Furthermore, spectral changes during pulse propagation are explicitly depicted in Fig. 4(d) with a spectral broadening of ∼38 nm corresponding to 3 dB points at the output. Moreover, it is observed that large phase accumulation due to excessive nonlinearity broadens the spectral waveform significantly with large ripples at the top without destabilizing the temporal pulse profile. In this context, it is to note that the periodic dispersion landscape of our designed HNBF does not induce any instability of the spectrum which might take place as reported earlier [47], [48]. Computations reveal that the ratio of the peak value of the dispersion to the average value i.e., $|\beta_{2peak}/\beta_{2avg}|$ ∼32 which is much larger than unity and thus restricts the pulse dynamics to strong dispersion management regime. Moreover, the pulse detuning $\Omega_k$ is much larger than the output spectrum with a negligible gain value which preserves the SS propagation. Fig. 5(a) shows the logarithmic plot of normalized power profile. The top-hat nature with steep vertical edges over 2 orders of magnitude is a clear signature of the pulse shape essentially being parabolic. Additionally, having included the propagation loss, we have compared the output temporal and spectral profiles as depicted in Fig. 5(a) and (b), respectively. In this context, we considered initially only the confinement loss (i.e., $4.5 \times 10^{-5}$ dB/m) which is almost negligible for our specific fiber design. In order to address the influence of loss due to 6 splices, we have neglected intrinsic losses assuming splicing of two fibers with identical geometries and mode field diameters, and considered only accumulated extrinsic loss of total 0.48 dB (i.e., maximum of 0.08 dB loss for each identical Bragg fiber splicing) [49]. Moreover, the material loss for the core only is taken to be 0.20 dB/m [50]. We have included these three types of losses in our fiber design and computation simultaneously and not separately as we have a highly nonlinear system. It is clear from Fig. 5 that incorporation of losses reduces only the energy content keeping pulse and spectrum shapes intact over a longer propagation length.

Realization of self-similar PPs over long distances in highly nonlinear passive optical fibers is restricted by few important factors. Soliton number $N$ gives a relative measurement of GVD and SPM effect and determines which effect to dominate the pulse evolution depending on the respective values of $L_D$ and $L_{NL}$. Moreover, influence of GVD is controlled by $L_D$ and to reduce the dispersive effect, lower $\beta_2$ values are required. On the other hand, high nonlinearity itself dictates a large value of $\gamma$ with a consequential smaller $L_{NL}$. PP formation is accomplished for a particular set of $\beta_2$ and $\gamma$ values. However, excessive nonlinearity fails to be balanced by present dispersion which results in separate role of GVD and SPM on pulse evolution leading to OWB. Thus, PPs are formed in such SPM dominated fibers with a much shorter self-similar propagation regime. Besides, dominating GVD again results in pulse distortions, further reshaping, etc. leading to absence of any desired self-similair regime. Our proposed scheme of passive modulation of dispersion around the zero dispersion value enhances the aforesaid self-similar propagation regime with consequential rapid nonlinear modulations over long distances. According to our fiber design, F1 is a dispersion-decreasing and nonlinearity-increasing fiber with $L_D$ varying over a wide range, from a few meters to several kilometers with $L_{NL}$ in the range of centimeters, thereby resulting in $N$ variation from

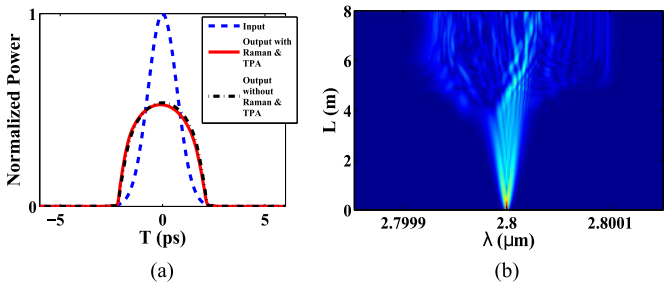


Fig. 6. (a) Temporal input and output profiles with the Raman effect and two-photon absorption effect accounting for nonlinear losses. (b) Spectral evolution of the pulse through the Bragg fiber in presence of TOD.

7 to 30 along the fiber length. Such variations in $\beta_2$ and $\gamma$ profiles dictate a gradual decrement of GVD effect, with a corresponding large nonlinearity which results in formation of efficient high power PPs within a very short HNBF length. In order to stabilize the so formed PPs over a longer propagation distance, $\beta_2$ is gradually reduced to a value close to zero in F2 and PPs are allowed to propagate through a rapidly varying longitudinal dispersion profile around nearly-zero average. Simultaneously the nonlinear coefficient has been modulated with a non-zero mean value. For F2-fiber-series, the mean of the rapid $\beta_2$ variation is around 0.005 $ps^2$/m which is maintained over a long propagation distance. Thus, GVD accumulated phase-shifts do not influence the temporal broadening of the pulse any further and hence we get a stable self-similar PP over long ranges. Moreover, the longitudinally modulated nonlinearity of the fiber only broadens the spectrum without destabilizing the temporal profile of the PP. For the entire fiber length $N$ is much greater than 10; in fact, due to the exceptional design of the fiber, $N$ varies with an average of $\sim$37 with peak power of the input pulse being 150 W.

The results shown so far are excluding the effect of higher order dispersion and nonlinear terms. Now we investigate the dynamics of the PPs under the effect of TOD and higher order nonlinearities. Firstly, the nonlinear terms relating effects like SRS and TPA have been included and the simulated results of (8) (excluding $\beta_3$ term) depicted in Fig. 6(a) clearly shows that higher order nonlinearities have negligible effects on pulse propagation while pumping in the normal dispersion regime (on an average) of the designed fiber for the considered waveguide parameters and chosen picosecond pulses of relatively low input power [29], [51], [52]. Moreover, the effect of TOD has been included in the present work, which surely have a deleterious impact on pulse propagation in practice. Fig. 6(b) shows the distortion in pulse propagation due to the inclusion of TOD in such a segmented Bragg fiber which limits the length of the stable PP propagation. A new approach to significantly reduce the TOD effect in such fibers beyond the proposed length is being developed with a transverse chirped fiber structure and will be presented elsewhere.

In order to establish the suitability of the counterpart alternating fiber segment for our purpose, we have compared the obtained results with the corresponding outcome from a counterpart single fiber segment. For this, we have adopted a single fiber segment with the same near mean-zero dispersion profile (as shown in Fig. 2(b)) stretching over the entire propagation length and observed the pulse evolution through it after the parabolic reshaping. Fig. 7 depicts the evolution of $M$ for both the alternating segment and the single fiber segment. A comparative study clearly states that for the single fiber segment, the input pulse transforms rapidly to PP attaining a lower $M$ value, and propagates almost self-consistently over a shorter distance of propagation than that obtained for the alternating segment. Moreover, the pulse propagation through the single fiber segment is more prone to higher order nonlinear effects (e.g., four wave mixing, modulation instability etc; Raman effect has been deliberately excluded in our design/performance due to unavailability of all the relevant parameters for the core material) and thus the length of the stable self-similar propagation regime is likely to be restricted. The periodically varying dispersion landscape along with corresponding modulation in nonlinearity has been adopted to avoid the higher order

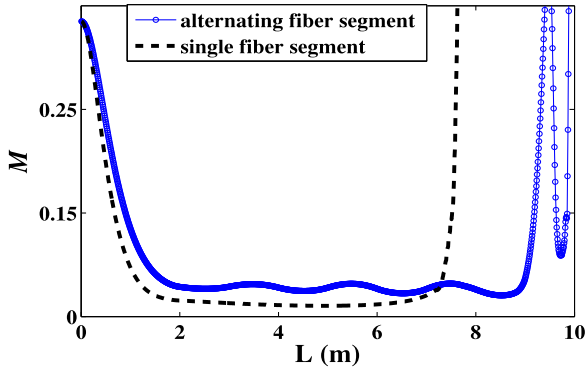


Fig. 7. Evolution of misfit parameter $M$ for both the counterpart alternating fiber segment (blue curve) and single fiber segment (black dashed curve)

phase-matching based nonlinear effects, however propagating pulse would feel a high N value required to maintain the self-similarity over a longer propagation distance.

## 5. Conclusion

In this paper, a novel scheme of rapidly varying longitudinal dispersion profile around a mean value close to zero with consequential simultaneous modulation in nonlinear coefficients, has been proposed in order to achieve self-similar stable propagation in passive fibers. To implement the proposed scheme, we have designed a *GeAsSe/AsSe* glass based highly nonlinear and segmented Bragg fiber. At 2.8 $\mu$m, a self-similar parabolic pulse with 4.12 $p$s FWHM and $\sim$38 nm of 3 dB spectral broadening for propagation over several meters of our designed fiber has been achieved numerically. Notably, sustained self-similarity of such parabolic pulses with propagation over longer lengths makes them suitable for potential applications in high power delivery and SC generaion. We claim this finding as first ever report self-similar propagation of such PPs after formation over a longer distance through a suitably designed passive fiber in the mid-IR.

## References

[1] A. Barh, S. Ghosh, G. P. Agrawal, R. K. Varshney, I. D. Aggarwal, and B. P. Pal, "Design of an efficient mid-ir light source using chalcogenide holey fibers: A numerical study," *J. Opt.*, vol. 15, no. 3, 2013, Art. no. 035205. [Online]. Available: http://stacks.iop.org/2040-8986/15/i=3/a=035205
[2] S. Jackson, "Towards high-power mid-infrared emission from a fibre laser," *Nature Photon.*, vol. 6, pp. 423–431, 2012.
[3] I. Ilev and R. Waynant, *Mid-Infrared Semiconductor Optoelectronics*, A. Krier, Ed. London, U.K.: Springer-Verlag, 2006.
[4] V. A. Serebryakov, E. V. Boko, N. N. Petrishchev, and A. V. Yan, "Medical applications of mid-ir lasers. Problems and prospects," *J. Opt. Technol.*, vol. 77, no. 1, pp. 6–17, Jan. 2010. [Online]. Available: http://jot.osa.org/abstract.cfm?URI=jot-77-1-6
[5] B. Eggleton, B. Luther-Davies, and K. Richardson, "Chalcogenide photonics," *Nature Photon.*, vol. 5, pp. 141–148, 2011.
[6] J. Sanghera and I. Aggarwal, "Active and passive chalcogenide glass optical fibers for ir applications: A review," *J. Non-Crys. Solids*, vol. 256, pp. 6–16, 1999.
[7] R. Wang *et al.*, "Identifying the best chalcogenide glass compositions for the application in mid-infrared waveguides," *Proc. SPIE*, vol. 9444, 2015, Art. no. 944406. [Online]. Available: http://dx.doi.org/10.1117/12.2074815
[8] A. Yang *et al.*, "GaSbS chalcogenide glasses for mid-infrared applications," *J. Amer. Ceram. Soc.*, vol. 99, no. 1, pp. 12–15, 2016.
[9] G. Barenblatt, *Scaling, Self-Similarity, and Intermediate Asymptotics: Dimensional Analysis and Intermediate Asymptotics*. Cambridge, U.K.: Cambridge Univ. Press, 1996.
[10] V. I. Kruglov, A. C. Peacock, and J. D. Harvey, "Exact self-similar solutions of the generalized nonlinear schrödinger equation with distributed coefficients," *Phys. Rev. Lett.*, vol. 90, Mar. 2003, Art. no. 113902. [Online]. Available: http://link.aps.org/doi/10.1103/PhysRevLett.90.113902

[11] T. Hirooka and M. Nakazawa, "Parabolic pulse generation by use of a dispersion-decreasing fiber with normal group-velocity dispersion," *Opt. Lett.*, vol. 29, no. 5, pp. 498–500, Mar. 2004. [Online]. Available: http://ol.osa.org/abstract.cfm?URI=ol-29-5-498
[12] D. Anderson, M. Desaix, M. Karlsson, M. Lisak, and M. L. Quiroga-Teixeiro, "Wave-breaking-free pulses in nonlinear-optical fibers," *J. Opt. Soc. Amer. B*, vol. 10, pp. 1185–1190, Jul. 1993.
[13] W. J. Tomlinson, R. H. Stolen, and A. M. Johnson, "Optical wave breaking of pulses in nonlinear optical fibers," *Opt. Lett.*, vol. 10, pp. 457–459, Sep. 1985.
[14] M. E. Fermann, V. I. Kruglov, B. C. Thomsen, J. M. Dudley, and J. D. Harvey, "Self-similar propagation and amplification of parabolic pulses in optical fibers," *Phys. Rev. Lett.*, vol. 84, pp. 6010–6013, Jun. 2000.
[15] V. I. Kruglov, A. C. Peacock, J. D. Harvey, and J. M. Dudley, "Self-similar propagation of parabolic pulses in normal-dispersion fiber amplifiers," *J. Opt. Soc. Amer. B*, vol. 19, no. 3, pp. 461–469, Mar. 2002.
[16] F. O. Ilday, J. R. Buckley, W. G. Clark, and F. W. Wise, "Self-similar evolution of parabolic pulses in a laser," *Phys. Rev. Lett.*, vol. 92, May 2004, Art. no. 213902. [Online]. Available: http://link.aps.org/doi/10.1103/PhysRevLett.92.213902
[17] F. Parmigiani *et al.*, "Ultra-flat spm-broadened spectra in a highly nonlinear fiber using parabolic pulses formed in a fiber bragg grating," *Opt. Exp.*, vol. 14, pp. 7617–7622, Aug. 2006.
[18] C. Finot, B. Barviau, G. Millot, A. Guryanov, A. Sysoliatin, and S. Wabnitz, "Parabolic pulse generation with active or passive dispersion decreasing optical fibers," *Opt. Exp.*, vol. 15, pp. 15824–15835, Nov. 2007.
[19] A. Chong *et al.*, "Pulse generation without gain-bandwidth limitation in a laser with self-similar evolution," *Opt. Exp.*, vol. 20, no. 13, pp. 14213–14220, Jun. 2012. [Online]. Available: http://www.opticsexpress.org/abstract.cfm?URI=oe-20-13-14213
[20] S. Lavdas, J. B. Driscoll, H. Jiang, R. R. Grote, R. M. Osgood, and N. C. Panoiu, "Generation of parabolic similaritons in tapered silicon photonic wires: Comparison of pulse dynamics at telecom and mid-infrared wavelengths," *Opt. Lett.*, vol. 38, pp. 3953–3956, Oct. 2013.
[21] A. Barh, S. Ghosh, R. Varshney, and B. Pal, "A tapered chalcogenide microstructured optical fiber for mid-ir parabolic pulse generation: Design and performance study," *IEEE J. Sel. Topics Quantum Electron.*, vol. 20, no. 5, pp. 590–596, Sep./Oct. 2014.
[22] C. Finot and S. Boscolo, "Parabolic similaritons in optical fibers," in *Odyssey of Light in Nonlinear Optical Fibers: Theory and Applications*. Boca Raton, FL, USA: CRC Press, 2015.
[23] P. Biswas, P. Adhikary, A. Biswas, and S. Ghosh, "Formation and stability analysis of parabolic pulses through specialty microstructured optical fibers at 2.1 $\mu$m," *Opt. Commun.*, vol. 377, pp. 120–127, 2016. [Online]. Available: http://www.sciencedirect.com/science/article/pii/S0030401816303996
[24] C. Finot, L. Provost, P. Petropoulos, and D. J. Richardson, "Parabolic pulse generation through passive nonlinear pulse reshaping in a normally dispersive two segment fiber device," *Opt. Exp.*, vol. 15, no. 3, pp. 852–864, Feb. 2007. [Online]. Available: http://www.opticsexpress.org/abstract.cfm?URI=oe-15-3-852
[25] S. O. Iakushev, O. V. Shulika, and I. A. Sukhoivanov, "Passive nonlinear reshaping towards parabolic pulses in the steady-state regime in optical fibers," *Opt. Commun.*, vol. 285, pp. 4493–4499, 2012.
[26] C. Finot, J. M. Dudley, B. Kibler, D. J. Richardson, and G. Millot, "Optical parabolic pulse generation and applications," *IEEE J. Quantum Electron.*, vol. 45, no. 11, pp. 1482–1489, 2009.
[27] A.Chong, L. Wright, and F. Wise, "Ultrafast fiber lasers based on self-similar pulse evolution: a review of current progress," *Rep. Prog. Phys.*, vol. 78, pp. 113901-1–113901-15, Oct. 2015.
[28] G. Agrawal, *Nonlinear Fiber Optics*. New York, NY, USA: Academic Press, 2007.
[29] C. Xiong *et al.*, "Characterization of picosecond pulse nonlinear propagation in chalcogenide $As_2S_3$ fiber," *Appl. Opt.*, vol. 48, no. 29, pp. 5467–5474, Oct. 2009. [Online]. Available: http://ao.osa.org/abstract.cfm?URI=ao-48-29-5467
[30] G. Jiang, Y. Fu, Y. Huang, and H. Chen, "Generation of the self-similar parabolic pulses by designing comb-like profiled dispersion fiber based on alternately arranged single-mode fibers and dispersion-shifted fibers," *Optik*, vol. 124, no. 22, pp. 5328–5331, 2013.
[31] D. Ghosh, D. Chowdhury, and M. Basu, "Silica based highly nonlinear fibers to generate parabolic self-similar pulses," *Opt. Quant. Electron.*, vol. 47, pp. 2615–2635, 2015.
[32] Infrared chalcogenide glass IRG 24, Advanced Optics, Schott AG, Mainz, Germany, 2016. [Online]. Available: http://www.schott.com/advanced_optics/english/download/schott-infrared- chalcog-glasses-irg24-january-2016-eng.pdf
[33] Infrared chalcogenide glass IRG 26, Advanced Optics, Schott AG, Mainz, Germany, 2016. [Online]. Available: http://www.schott.com/advanced_optics/english/download/schott-infrared- chalcog-glasses-irg26-january-2016-eng.pdf
[34] I. Kubat *et al.*, "Mid-infrared supercontinuum generation to 12.5$\mu$m in large na chalcogenide step-index fibres pumped at 4.5$\mu$m," *Opt. Exp.*, vol. 22, no. 16, pp. 19169–19182, Aug. 2014. [Online]. Available: http://www.opticsexpress.org/abstract.cfm?URI=oe-22-16-19169
[35] C. Finot, "Dispersion managed self-similar parabolic pulses," *J. Opt. A, Pure Appl. Opt.*, vol. 10, no. 8, 2008, Art. no. 085101. [Online]. Available: http://stacks.iop.org/1464-4258/10/i=8/a=085101
[36] S. Ghosh, R. K. Varshney, B. P. Pal, and G. Monnom, "A bragg-like chirped clad all-solid microstructured optical fiber with ultra-wide bandwidth for short pulse delivery and pulse reshaping," *Opt. Quantum Electron.*, vol. 42, no. 1, pp. 1–14, 2010. [Online]. Available: http://dx.doi.org/10.1007/s11082-010-9417-8
[37] D.-I. Yeom, E. C. Mägi, M. R. E. Lamont, M. A. F. Roelens, L. Fu, and B. J. Eggleton, "Low-threshold supercontinuum generation in highly nonlinear chalcogenide nanowires," *Opt. Lett.*, vol. 33, no. 7, pp. 660–662, Apr. 2008. [Online]. Available: http://ol.osa.org/abstract.cfm?URI=ol-33-7-660
[38] E. C. Mägi, L. B. Fu, H. C. Nguyen, M. R. E. Lamont, D. I. Yeom, and B. J. Eggleton, "Enhanced kerr nonlinearity in sub-wavelength diameter $As_2Se_3$ chalcogenide fiber tapers," *Opt. Exp.*, vol. 15, no. 16, pp. 10324–10329, Aug. 2007. [Online]. Available: http://www.opticsexpress.org/abstract.cfm?URI=oe-15-16-10324
[39] L. Brilland *et al.*, "Fabrication of complex structures of holey fibers in chalcogenide glass," *Opt. Exp.*, vol. 14, no. 3, pp. 1280–1285, Feb. 2006. [Online]. Available: http://www.opticsexpress.org/abstract.cfm?URI=oe-14-3-1280

[40] A. I. Latkin, S. K. Turitsyn, and A. A. Sysoliatin, "Theory of parabolic pulse generation in tapered fiber," *Opt. Lett.*, vol. 32, no. 4, pp. 331–333, Feb. 2007. [Online]. Available: http://ol.osa.org/abstract.cfm?URI=ol-32-4-331
[41] Y. Sun *et al.*, "Fabrication and characterization of multimaterial chalcogenide glass fiber tapers with high numerical apertures," *Opt. Exp.*, vol. 23, no. 18, pp. 23472–23483, Sep. 2015. [Online]. Available: http://www.opticsexpress.org/abstract.cfm?URI=oe-23-18-23472
[42] M. Jelinek, V. Hlavaty, J. Hrabina, and B. Mikel, "Splicing and shaping of the special optical fibers," *Proc. SPIE*, vol. 10231, 2017, Art. no. 102311Y. [Online]. Available: http://dx.doi.org/10.1117/12.2265771
[43] C. Wei, X. Zhu, R. A. Norwood, and N. Peyghambarian, "Passively continuous-wave mode-locked $Er^{3+}$-doped ZBLAN fiber laser at 2.8 $\mu$m," *Opt. Lett.*, vol. 37, no. 18, pp. 3849–3851, Sep. 2012. [Online]. Available: http://ol.osa.org/abstract.cfm?URI=ol-37-18-3849
[44] C. Petersen *et al.*, "Mid-infrared supercontinuum covering the 1.4–13.3 $\mu$m molecular fingerprint region using ultra-high na chalcogenide step-index fibre," *Nature Photon.*, vol. 8, 2014, Art. no. 830834.
[45] Y. Yu *et al.*, "1.8-10m mid-infrared supercontinuum generated in a step-index chalcogenide fiber using low peak pump power," *Opt. Lett.*, vol. 40, no. 6, pp. 1081–1084, Mar. 2015. [Online]. Available: http://ol.osa.org/abstract.cfm?URI=ol-40-6-1081
[46] B. Zhang *et al.*, "High brightness 2.2–12 $\mu$m mid-infrared supercontinuum generation in a nontoxic chalcogenide step-index fiber," *J. Amer. Ceram. Soc.*, vol. 99, no. 8, pp. 2565–2568, 2016. [Online]. Available: http://dx.doi.org/10.1111/jace.14391
[47] M. Droques, A. Kudlinski, G. Bouwmans, G. Martinelli, and A. Mussot, "Experimental demonstration of modulation instability in an optical fiber with a periodic dispersion landscape," *Opt. Lett.*, vol. 37, no. 23, pp. 4832–4834, Dec. 2012. [Online]. Available: http://ol.osa.org/abstract.cfm?URI=ol-37-23-4832
[48] C. Finot, J. Fatome, A. Sysoliatin, A. Kosolapov, and S. Wabnitz, "Competing four-wave mixing processes in dispersion oscillating telecom fiber," *Opt. Lett.*, vol. 38, no. 24, pp. 5361–5364, Dec. 2013. [Online]. Available: http://ol.osa.org/abstract.cfm?URI=ol-38-24-5361
[49] B. Bourliaguet, C. Paré, F. Émond, A. Croteau, A. Proulx, and R. Vallée, "Microstructured fiber splicing," *Opt. Exp.*, vol. 11, no. 25, pp. 3412–3417, Dec. 2003. [Online]. Available: http://www.opticsexpress.org/abstract.cfm?URI=oe-11-25-3412
[50] Z. Tang *et al.*, "Low loss Ge-As-Se chalcogenide glass fiber, fabricated using extruded preform, for mid-infrared photonics," *Opt. Mater. Exp.*, vol. 5, no. 8, pp. 1722–1737, Aug. 2015. [Online]. Available: http://www.osapublishing.org/ome/abstract.cfm?URI=ome-5-8-1722
[51] S. Vyas, T. Tanabe, G. Singh, and M. Tiwari, "Broadband supercontinuum generation and raman response in $Ge_{11.5}As_{24}Se_{64.5}$ based chalcogenide photonic crystal fiber," in *Proc. 2016 Int. Conf. Comput. Techn. Inf. Commun. Technol.*, Mar. 2016, pp. 607–611.
[52] R. E. Slusher, G. Lenz, J. Hodelin, J. Sanghera, L. B. Shaw, and I. D. Aggarwal, "Large raman gain and nonlinear phase shifts in high-purity $As_2Se_3$ chalcogenide fibers," *J. Opt. Soc. Amer. B*, vol. 21, no. 6, pp. 1146–1155, Jun. 2004. [Online]. Available: http://josab.osa.org/abstract.cfm?URI=josab-21-6-1146